Atmos. Chem. Phys. Discuss., 10, 1483–1516, 2010
www.atmos-chem-phys-discuss.net/10/1483/2010/

Atmospheric Chemistry and Physics Discussions

This discussion paper is/has been under review for the journal Atmospheric Chemistry and Physics (ACP). Please refer to the corresponding final paper in ACP if available.

Tropospheric ozone variations at the Nepal climate observatory – pyramid (Himalayas, 5079 m a.s.l.) and influence of stratospheric intrusion events

P. Cristofanelli[1], A. Bracci[1,2], M. Sprenger[2], A. Marinoni[1], U. Bonafè[1], F. Calzolari[1], R. Duchi[1], P. Laj[3], J. M. Pichon[4], F. Roccato[1], H. Venzac[4], E. Vuillermoz[5], and P. Bonasoni[1,5]

[1]Institute for Atmospheric Science and Climate, National Research Council, Bologna, Italy
[2]ETHZ, Zurich, Switzerland
[3]Lab. de Glaciologie et Géophysique de l'Environnement, St Martin d'Hères Cedex, France
[4]Lab. de Meteorologie Physique, CNRS, Université Blaise Pascal, Aubiere Cedex, France
[5]EV-K[2]-CNR Committee, 24126 Bergamo, Italy

Received: 21 December 2009 – Accepted: 7 January 2010 – Published: 20 January 2010

Correspondence to: P. Cristofanelli (p.cristofanelli@isac.cnr.it)

Published by Copernicus Publications on behalf of the European Geosciences Union.

Abstract

The paper presents the first 2-years of continuous surface ozone (O_3) observations and systematic assessment of the influence of stratospheric intrusions (SI) at the Nepal Climate Observatory at Pyramid (NCO-P; 27°57′ N, 86°48′ E), located in the Southern Himalayas at 5079 m a.s.l. Continuous O_3 monitoring has been carried out at this GAW-WMO station in the framework of the Ev-K2-CNR SHARE and UNEP ABC projects since March 2006. Over the period March 2006–February 2008, an average O_3 value of 49±12 ppbv (±1δ) was recorded, with a large annual cycle characterized by a maximum during the pre-monsoon (61±9 ppbv) and a minimum during the monsoon (39±10 ppbv). In general, the average O_3 diurnal cycles had different shapes in the different seasons, suggesting an important interaction between the synoptic-scale circulation and the local mountain wind regime.

Short-term O_3 behaviour in the middle/lower troposphere (e.g. at the altitude level of NCO-P) can be significantly affected by deep SI which, representing the most important natural input for tropospheric O_3, can also influence the regional atmosphere radiative forcing. To identify days possibly influenced by SI at the NCO-P, analyses were performed on in-situ observations (O_3 and meteorological parameters), total column O_3 data from OMI satellite and air-mass potential vorticity provided by the LAGRANTO back-trajectory model. In particular, a specially designed statistical methodology was applied to the time series of the observed and modelled stratospheric tracers. On this basis, during the 2-year investigation, 14.1% of analysed days were found to be affected by SI. The SI frequency showed a clear seasonal cycle, with minimum during the summer monsoon (1.2%) and higher values during the rest of the year (21.5%). As suggested by the LAGRANTO analysis, the position of the subtropical jet stream could play an important role in determining the occurrence of deep SI transport on the Southern Himalayas.

In order to estimate the fraction of O_3 due to air-mass transport from the stratosphere at the NCO-P, the 30 min O_3 concentrations recorded during the detected SI days were

ACPD

10, 1483–1516, 2010

analysed. In particular, in-situ relative humidity and black carbon observations were used to exclude influence from wet and polluted air-masses transported by up-valley breezes. This analysis led to the conclusion that during SI O_3 significantly increased by 27.1% (+13 ppbv) with respect to periods not affected by such events. Moreover, the integral contribution of SI (O_{3S}) to O_3 at the NCO-P was also calculated, showing that 13.7% of O_3 recorded at the measurement site could be attributed to SI. On a seasonal basis, the lowest SI contributions were found during the summer monsoon (less than 0.1%), while the highest were found during the winter period (24.2%). These results indicated that, during non-monsoon periods, high O_3 levels could affect NCO-P during SI, thus influencing the variability of tropospheric O_3 over the Southern Himalayas. Being a powerful regional greenhouse gas, these results indicate that the evaluation of the current and future regional climate cannot be assessed without properly taking into account the influence of SI to tropospheric O_3 in this important area.

1 Introduction

Even if about 90% of atmospheric O_3 molecules resides in the stratosphere, tropospheric O_3 strongly influences the radiative budget of the atmosphere (Forster et al., 2007) and the oxidation capacity of the troposphere (Gauss et al., 2003). Due to its high chemical reactivity in the lower troposphere, O_3 is considered a dangerous pollutant, causing harm to human health (e.g., Hoek et al., 1993; Conti et al., 2005) and ecosystems (e.g., Fuhrer and Booker, 2003; Paoletti et al., 2006), while in the free troposphere it has been recognised as the third greenhouse gas in terms of anthropogenic radiative forcing (Forster et al., 2007). Although the greatest contribution to tropospheric O_3 today comes from photochemical production (e.g., Jacobson, 2002), other concurring processes like Stratosphere-Troposphere Exchange (STE) cannot be neglected (e.g., Wild, 2007). As a result of the interaction of these processes with air-mass transport (both regional and long range), and due to its variable chemical lifetime (from days to a month), tropospheric O_3 exhibits complex spatial and temporal

ACPD
10, 1483–1516, 2010

variations that lead to an inhomogeneous distribution of its radiative forcing (Mickley et al., 2004) and non-linear effects on regional air quality (West et al., 2009). Thus, it is crucial to evaluate in detail the processes able to influence O_3 behaviour. Due to the increasing emissions of anthropogenic O_3 precursors (Ohara et al., 2007), the issue appears especially urgent with regard to South Asia, where a vast region extending from the Indian Ocean to the Himalayas is characterised by the presence of copious amounts of aerosol and pollutant gases (the so-called Asian Brown Cloud), with severe implications on regional climate, air-quality and food safety (Ramanathan et al., 2008). In particular, there is still a gap in knowledge concerning the typical levels and variations of tropospheric O_3 over the high Himalayas where, besides influencing the mountain ecosystem air quality, it can strongly contribute to the atmospheric heating of absorbing aerosols in the Asian Brown Cloud (Ramanathan et al., 2008).

For these reasons and with purpose of contributing to filling this gap in knowledge, this work presents a systematic evaluation of the role of stratospheric air-mass transport in determining the O_3 levels observed at the WMO – GAW station "Nepal Climate Observatory – Pyramid" (NCO-P, 5079 m a.s.l., Nepal). At this station, in the framework of the UNEP ABC (Atmospheric Brown Clouds) and Ev-K2-CNR SHARE (Stations at High Altitude for Research on the Environment) projects, since March 2006 high quality continuous measurements of trace gases, aerosol and meteorological parameters have been continuously conducted, in order to attain a detailed characterization of the background tropospheric composition and variability over the remote South Himalayas. Thus, together with future work that will focus on polluted air-mass transport, the present paper better clarifies the role played by transport processes in determining the O_3 levels and variability in one of the most critical high-altitude regions. Moreover, this experimental investigation can also provide useful hints for better evaluating the capacity of global and regional models in assessing the current tropospheric O_3 levels, and its climatic effect in this important world area. In fact, high mountain stations are appropriate locations for investigating the episodic transport of stratospheric air-masses deep into the troposphere (e.g., Elbern et al., 1997; Stohl et al., 2000), as well as

representing very suitable sites for the study tropospheric background conditions (e.g., Wotawa et al., 2000; Henne et al., 2008). Signal of stratospheric air-masses have been detected by Wang et al. (2006) by analysing O_3 and CO values recorded during a summer campaign in the northeastern Qinghai-Tibetan Plateau (Mt. Waliguan, 26.3° N, 100.9° E, 3816 m a.s.l.). At the same measurement site, by analysing case studies, Ding and Wang (2006) suggested that STE can play an important role during summer but without providing any estimate of the possible contribution to O_3 levels. Concerning the Mt. Everest region, by analysing single case studies and long-term satellite measurements, Moore and Sample (2004) indicated that SI can trigger extreme weather events at the mountain peak, also speculating that the interaction of the Tibetan Plateau with large-scale circulation can favour STE over South Himalayas (Moore and Semple, 2005). By analysing data from two field campaigns, Zhu et al. (2006) suggested that high O_3 in the northern slope of Mt. Everest could be attributed to katabatic winds pumping down O_3 rich air-masses from upper air levels. More recently, by analysing the first round-year of continuous O_3 measurement at NCO-P, Cristofanelli et al. (2009) evaluated that during 25 SI days the daily O_3 mixing ratio increased by 9.3% compared to seasonal values.

To detect experimentally stratospheric intrusion (SI) events at a specific surface measurement site or throughout the troposphere, the temporal variations of specific stratospheric tracers can be analysed. SI is often related to frontal activity, leading to the development of tropopause folds (e.g., Sprenger et al., 2003), deep troughs (e.g., Davies and Schuepbach, 1994) and cut-off lows (e.g., Sprenger et al., 2007) at upper levels, as well as rapid cyclones (e.g., Loring et al., 1996), fronts or high-pressure systems at the surface (e.g., Davies and Schuepbach, 1994). For this reason, concomitant atmospheric pressure (AP) variations are often observed at measurement sites when SI occurs. Several authors (e.g., Sprenger et al., 2007) have used Ertl's potential vorticity (PV) to diagnose the presence of stratospheric air deep into the troposphere. In fact, in the atmosphere above 350 hPa, PV rapidly increases with altitude, reaching typical values above 1.0 pvu (Danielsen, 1968) at the tropopause level (where

ACPD
10, 1483–1516, 2010

1 pvu=10^{-6} m^2 K kg^{-1} s^{-1}), thus representing a valid stratospheric tracer under adiabatic and frictionless flows. The detection of high values of total column ozone (TCO) over a specific location or the identification of strong TCO horizontal gradients can also be used to identify SI (e.g., Olsen et al., 2000; Wimmers et al., 2004).

Along with high O_3 concentrations and PV values, stratospheric air is also characterised by low water vapour contents and low anthropogenic pollutants (e.g. black carbon). For this reason the experimental recognition of SI at high mountain sites is often additionally based on the identification of "clean" and low RH conditions (e.g., Stohl et al., 2000; Trickl et al., 2009).

The work presents and analyses surface O_3 measurements continuously recorded at NCO-P from 1 March 2006 to 18 February 2008. In particular, by applying a specially designed selection methodology based on the analysis of in-situ data (O_3, AP, RH), satellite TCO data and 3-D air-mass back-trajectories, the days possibly influenced by SI were accurately identified. Here we extend the previous work by Cristofanelli et al. (2009) with the principal aim of further investigating SI seasonal cycle and estimating the SI contribution to the O_3 levels observed in South Himalayas.

2 Methods

2.1 Measurement site and in-situ observations

The NCO-P(27°57′ N, 86°48′ E) is located at 5079 m a.s.l., in the Southern Himalayas (Fig. 1) at the confluence of two glacial valleys: Lobuche and Khumbu. As shown by Bonasoni et al. (2010), the air-mass circulation at this measurement site is strongly influenced both by the synoptic scale circulation and the local mountain wind regime. The interaction between these components leads to the onset and decay of the summer monsoon and winter season reported by Bonasoni et al. (2010) and adopted also in this work to define seasonal transitions during the years (Table 1). In particular, up-valley breezes can favour the transport of polluted air-masses rich in O_3 and BC from lower

altitude regions. For this reason, particular attention was devoted to ensuring that the O_3 levels observed during the identified SI days were not influenced by anthropogenic emissions. In particular, as shown in Sect. 5 below, surface O_3 data were analysed as a function of RH and black carbon (BC), to prevent moist and polluted air-masses influencing the analysed measurements. Surface O_3 measurements (Fig. 2) have been continuously performed with a UV-photometric analyser (Thermo Scientific – Tei 49C), adopting the sampling procedures suggested within the GAW-WMO (GAW, 1992). During a maintenance campaign in February 2007, the instrument was compared against a travelling standard by GAW/WCC at EMPA (World Calibration Centre for Surface Ozone, Carbon Monoxide and Methane at the Swiss Federal Laboratories for Materials Testing and Research). In agreement with Klausen et al. (2003), the combined standard uncertainty was ascertained to be less than ±1.5 ppbv in the range 0–100 ppbv. At NCO-P, equivalent BC concentrations are determined using a multi-angle absorption photometer (MAAP 5012, Thermo Electron Corporation). This instrument measures the absorption coefficient of aerosol deposited on a glass fibre filter tape, also removing the scattering effect at different angles, which can interfere with optical absorption measurements. The reduction of light transmission at 670 nm, multiple reflection intensities, and air sample volume are continuously integrated over the sample run period to provide a real time output (1 min resolution) of equivalent BC concentration (Petzold et al., 2002). For further details on BC measurements and typical behaviours at NCO-P, please refer to Marinoni et al. (2010). At NCO-P, conventional meteorological parameters are continuously recorded by means of an integrated weather station (Vaisala WXT-410). In particular, AP shows a small variability during the year (standard deviation: 3.6 hPa) with an average value of 550.9 hPa. As shown in Fig. 2, the yearly AP cycle was characterised by higher (and less variable) values from June to October (552.2±0.6 hPa) and lower (and more variable) values from November to March (547.7±3.1 hPa). This behaviour appeared to be strongly affected by the so-called "Tibetan High", a strong thermal anticyclone forming in the upper troposphere during the monsoon season, while for the rest of the year the passage of eastward propa-

gating synoptic disturbances mainly determine AP variations at the measurement site (Böhner, 2006). All the in-situ parameters presented in this paper are reported at local time (LT, i.e. UTC+5:45 h), unless otherwise reported, while all concentrations refer to STP conditions.

2.2 Back-trajectory calculation

In order to determine the origin of air masses reaching NCO-P, 5-day back-trajectories starting at the measurement site were calculated every 6 h (at 00:00, 06:00, 12:00 and 18:00 UTC) with the Lagrangian Analysis Tool LAGRANTO (Wernli and Davies, 1997). To minimize possible effects of the differences between model and real topography, the 3-D trajectories were started at the pressure level of 530 hPa, which almost corresponds to the station height above sea level. Trajectory calculations were based on the 6-hourly meteorological 3-D grid field composing the operational analysis produced by the European Centre for Medium Range Weather Forecasts (ECMWF). The 3-D wind fields were interpolated onto a horizontal $1^{\circ} \times 1^{\circ}$ grid. Subgrid scale processes, like convection and turbulent diffusion, are not represented by LAGRANTO back-trajectories. To compensate partially for such uncertainties, and also to evaluate the coherence of flow, which depends strongly on the 3-D flow structure and temporal evolution, in addition to the backward trajectory started at the NCO-P location, 6 additional back-trajectories with endpoints shifted by $\pm 1^{\circ}$ in latitude/longitude and ±50 hPa in pressure were also considered.

For every point along the trajectory (interpolated at a time resolution of 2 h), the model provides the geographic location and altitude of the air parcel, as well as other important physical quantities, like Ertel's PV, which can facilitate the identification of stratospheric air-masses. For each analysed day, the highest PV values along the back-trajectories are shown in Fig. 2. It is evident that the highest PV values related to air-masses reaching the measurement site from October to mid-June, with lower values during the monsoon season.

ACPD
10, 1483–1516, 2010

2.3 Ozone Monitoring Instrument (OMI) data

Daily total column O_3 (TCO) from the Dutch-Finnish Ozone Monitoring Instrument (OMI) (Levelt et al., 2006a, b) on board the NASA Earth Observing System Aura satellite (Schoeberl et al., 2006) were analysed for the NCO-P location (pixel extension: 1.00° Lat.×1.25° Long.; local time overpass: ∼12:00 LT). In particular, TCO showed a clear seasonal behaviour (Fig. 2) characterized by low values from late September to early January (255±11 DU) and high values during the pre-monsoon period (278±13 DU). These variations are related to different controlling factors (Han et al., 2001; Tian et al., 2008): i.e. variations of large scale circulation, eddy transport, and chemical sources/sinks (Miyazaki et al., 2005).

3 Surface O_3 behaviour at NCO-P

The O_3 measurements at NCO-P represent the longest continuous O_3 time series recorded at an high-altitude Himalayan location. For the considered period, the surface O_3 mean concentrations gave a value of 49±12 ppbv; *N*:696 (±1σ; *N* being the number of data). As shown by the analysis of daily mean values (Fig. 3), the seasonal cycle of O_3 showed maxima during pre-monsoon periods (average mean value: 61±9 ppbv; *N*:202) and minima during the monsoon seasons (39±10 ppbv; *N*:247). The spring (pre-monsoon) maximum with a summer (monsoon) minimum is typical for seasonal O_3 cycles at other locations in South/South-East Asia (e.g., Wahid et al., 2001; Tanimoto et al., 2005; Agrawal et al., 2008), where the monsoon regime strongly influences atmospheric circulation. As shown by Bonasoni et al. (2010), while the seasonal O_3 minima during the monsoon period are related to the northward transport of air masses poor in O_3 from the Indian subcontinent and ocean, other processes can contribute to explaining the higher O_3 levels recorded during the remaining seasons. In particular, during the pre-monsoon period, both SI and long-range/regional transport from Central Asia, North Africa and Middle East (Wang et al., 2006; Sudo and Akimoto, 2007;

ACPD
10, 1483–1516, 2010

Bonasoni et al., 2010) can contribute to the observed O_3 concentrations. In addition to long-range transport, a not-negligible source of O_3 may also be the local/regional transport of air-masses rich in anthropogenic pollutants and biomass burning products (Bonasoni et al., 2008). In fact, the efficient valley wind circulation characterising the Khumbu region represents a favoured channel for the injection of pollution to the high Himalayas (Bonasoni et al., 2010). The influence of the mountain wind regimes on O_3 concentrations was investigated by considering the average diurnal variation of normalized O_3 values obtained by subtracting daily means from the actual 30 min O_3 concentrations (Fig. 4). In general, the average O_3 diurnal cycles presented different shapes for the different seasons. During the winter season, a day-time minimum (16:00–17:00) and a night-time maximum (04:00–05:00) were observed with a diurnal cycle amplitude of 3.6 ppbv. The average behaviour of the in-situ meridional wind component (V_y), clearly indicated that up-valley winds (V_y>0 m/s) usually dominated during day-time and down-valley winds (V_y<0 m/s) during night-time. This suggests that the day-time O_3 minimum can be attributed to the advection of air-masses from the ABL, which, due to surface dry deposition and enhanced titration, could be characterised by lower O_3 concentrations with respect to air-masses more representative of the free troposphere. On the other hand, the day-time O_3 minimum might also be due to O_3 loss by surface deposition along the valley floor or in-situ photochemical destruction under low nitrogen oxide (NO_x) conditions, which are likely at high-mountain sites (e.g. Fischer et al., 2003; Henne et al., 2008). During the pre-monsoon season, even though a marked diurnal wind breeze cycle was present at NCO-P, no significant average O_3 diurnal variation was observed. This probably indicated that during this season the contribution of air-masses transported from the lower troposphere by up-valley breezes almost equal the contribution of air-masses coming from the upper troposphere via down-valley breezes. During the summer monsoon, a significant O_3 maximum was observed at 10:00–11:00 with a minimum in the evening (at 20.00–21:00) and a diurnal cycle amplitude of 2.8 ppbv. This behaviour suggests the influence of a weak local photochemical O_3 production, probably related to a more efficient transport of O_3 precursor

ACPD
10, 1483–1516, 2010

favoured by the less stable atmospheric conditions during summer. In fact, O_3 concentrations decreased from 12:00, when cumulus formation usually developed at NCO-P (Bonasoni et al., 2010) reducing incoming solar radiation. O_3 reached a minimum concentration on 20:00–21:00, suggesting that destruction processes and/or surface deposition are dominant. The slightly higher O_3 levels observed during night-time were probably more representative for air-masses advected to NCO-P by the "large-scale" monsoon circulation (Bonasoni et al., 2010). In the post-monsoon season, the average O_3 diurnal cycle was characterised by a morning maximum (from 08:00 to 12:00) and a late afternoon minimum (18:00),with a diurnal cycle amplitude of 5.1 ppbv. Again, the low O_3 values during the afternoon were probably due to the transport of air-masses from the lower troposphere by up-valley winds (V_y>0). On the other hand, comparing the average diurnal variations of O_3 and V_y, it is likely that the morning O_3 maximum could be the result of different contributions. In fact, O_3 concentrations peaked both under down-valley (at 08:00 LT) and up-valley (at 10:00–11:00 LT) breezes. While the first "bump" in the average O_3 peak was probably related to clean air-masses from the upper/free troposphere (as also suggested by the low BC average values of 50 ng/m^3, see Marinoni et al., 2010), the second O_3 "bump" was probably related to air-masses mixed by the developing up-valley breezes (as also suggested by the BC concentrations increasing from 50 to 200 ng/m^3, see Marinoni et al., 2010). In fact, as shown by Venzac et al. (2008), during the post-monsoon season ultrafine (d_p of 10 nm or less) particle concentrations strongly increase after 11:00 LT, indicating new particle formation at the interface between ABL and "free tropospheric" air-masses.

4 Climatological analysis of stratospheric intrusion at NCO-P

4.1 Identification of stratospheric intrusions at the NCO-P

For the purpose of identifying SI at NCO-P, different selection criteria were applied, according to the methodology presented by Cristofanelli et al. (2009). The detection

algorithm was based on the analysis of in-situ O_3, AP and RH, satellite-derived TCO daily values, and PV calculated along air-mass back-trajectories. In particular, days were selected that were characterised by the presence of air-masses with PV values exceeding the WMO definition of dynamical tropopause (i.e. PV>1.6 pvu, see WMO, 1986), and by significant variations of daily O_3, AP and TOC values over their seasonal cycles, as evaluated by applying a three-time repeated 19-day running mean (the so-called "Kolmogorov–Zurbenko" filter, see Sebald et al., 2000). As shown by previous investigations (Eisele et al., 1999; Zanis et al., 1999; Trickl et al., 2009), the downward transport of the stratospheric air-masses deep into the troposphere can be very complex, often leading to strong mixing between stratospheric and tropospheric air. In fact, only in a few very spectacular SI (see e.g., Bonasoni et al., 1999; Stohl et al., 2000) did all the tracers showed "clear" stratospheric signatures. Thus, different selection criteria were adopted in order to take into account expressly the possible mixing of stratospheric air-masses within the troposphere. In particular, a specific day was considered as being influenced by SI if enhanced daily O_3 mixing ratio was found and at least one of the following criteria was fulfilled:

- significant variations of daily AP value AND the presence of back-trajectories with PV>1.6 pvu;
- presence of back-trajectories with PV>1.6 pvu AND significant TCO daily value increases;
- significant variations of daily AP values AND significant TCO daily value increases.

Based on this methodology, among the 695 days for which data were available, 44 days (6.3% of the data-set) were retained as probably influenced by SI. However, it should be noted that several studies (e.g., Schuepbach et al., 1999; Zachariasse at al., 2000; Ding and Wang, 2006) stressed the importance of "sub-synoptic" processes (e.g. shear-induced differential advection or clear-air turbulence) in favouring the descent of

stratospheric air-masses down to the middle troposphere. Moreover, Zhu et al. (2006) suggested that mountain katabatic wind can favour the descent of air-masses from the upper troposphere to a glacial valley near Mt. Everest. For these reasons and with the purpose of selecting the SI events related to downward transport not associated with coherent airstreams, those days were also identified for which the following criteria are simultaneously fulfilled: (i) the daily 30 min O_3 maximum was higher than the seasonal cycle (as deduced by applying the Kolmogorov–Zurbenko filter); (ii) 30 min RH data showed values lower than 60%, a threshold that can still be considered representative for the intrusion of stratospheric air into the troposphere (e.g., Trickl et al., 2009); (iii) there is a negative significant correlation (as deduced by applying a simple linear least-square regression on a 24 h basis) between 30 min values of O_3 and RH; (iv) at least one among AP, PV and TOC daily values showed significant variations with respect to their seasonal cycles (as deduced by applying the Kolmogorov–Zurbenko filter). Applying these criteria, a further 54 days (7.8% of the analysed period) were retained as influenced by SI. As resulting from the previous selection methodology, a total of 98 days were likely to be influenced by SI at NCO-P, which represents 14.1% of the investigated period. This indicated that a not-negligible fraction of time may be under the influence of stratospheric-influenced air-masses at the measurement site

4.2 Seasonal frequency of stratospheric intrusions at NCO-P

Figure 5 shows the seasonal frequency of the number of days possibly affected by SI during the investigated period as deduced from the applied selection methodology. The highest seasonal SI frequency was recorded during non-monsoon seasons and in particular during the dry season 2007 (27% of the period). High frequency values were also recorded for the post-monsoon (25%) and pre-monsoon 2007 (23%). The lowest SI seasonal frequencies were detected during the monsoon seasons (less that 2%). As also suggested by the LAGRANTO atmospheric circulation analysis (Bonasoni et al., 2010), such behaviour probably reflects the role of the SJS in promoting deep SI in the Southern Himalayas. In fact, while during the summer monsoon the SJS

was positioned on the northern side of the Tibetan Plateau (Schiemann et al., 2009), from October to May the axis of the SJS was situated between 25–30° N, thus being more likely to interact with the Himalayas. As deduced from the analysis, in general, during the 2-year investigation no evident inter-annual variability of SI frequency was recorded at NCO-P (Fig. 5). Only for the post-monsoon seasons, was an evident variation of SI frequency observed from 2006 (SI frequency: 15%) to 2007 (SI frequency: 25%). By analysing the synoptic-scale air-mass circulation at NCO-P by means of the 3-D air-mass back-trajectory clusters presented by Bonasoni et al. (2010), it was found that during the post-monsoon 2007, the synoptic scale circulation was more influenced by fast-moving westerly air-masses originating over North Africa (W-NA cluster) than during the post-monsoon 2006 (31% versus 11% of occurrences). In agreement with Schiemann et al., (2009), who pointed out an elevated interannual variability for the SJS occurrence during autumn, this further indicated that strong westerly flows possibly related with the SJS can play an important role in determining SI in the Southern Himalayas, even during the post-monsoon season. The leading role of SJS in favouring the transport of stratospheric air-masses to South Himalayas, is further described in a companion paper (Cristofanelli et al., 2010) presenting the principal synoptic scenarios (i.e. upper tropospheric sub-tropical fronts, westerly moving disturbances, quasi-stationary ridges) promoting SI at the NCO-P during non-monsoon periods.

5 Influence of stratospheric intrusions on O_3 concentrations at NCO-P

During SI the stratospheric air-masses intruding into the troposphere are mixed with tropospheric air. In order to retain only the measurement periods actually influenced by stratospheric air-masses, for each day identified as influenced by SI, the 30 min RH and BC behaviours were analysed. In particular, to prevent photochemical O_3 in polluted air-masses transported by up-valley flows to NCO-P from influencing the estimate of "stratospheric" O_3, only those observations were considered that were characterised by RH<60% and BC<166 ng/m^3 (the 75th percentile of the yearly BC observations at

NCO-P, see Marinoni et al., 2010). Based on this screening, during the 2-year periods (15 710 h) a total of 1591 h (10% of the analysed time period) were retained. If one assumes that during these periods the observed O_3 is entirely transported from the stratosphere, a rough estimate can be inferred as to the contribution of SI in determining the tropospheric O_3 levels in the Southern Himalayas. The seasonal O_3 concentrations associated with SI showed the highest values during the pre-monsoon 2006 (70±8 ppbv, *N*:550) and dry season 2007 (64±9 ppbv, *N*:562), with a cycle which resembles the typical yearly O_3 variations observed at the measurement site (Fig. 6). On average, a mean O_3 concentration of 61±9 ppbv (*N*=3831) was observed, corresponding to a significant excess of +27.1% (+13 ppbv), compared to periods not affected by SI. The seasonal net O_3 increase (expressed as percentage) recorded during SI with respect to periods not affected by such phenomena (Table 2) shows a seasonal cycle with the highest values during the post-monsoon (+22.0%, equivalent to +10 ppbv) and the lowest during the pre-monsoon (+8.6%, equivalent to +5 ppbv). It is worth noting that the small average O_3 increases were observed during the pre-monsoon seasons, which could seem in contrast with the high average O_3 concentrations recorded during this season for SI (Table 2). However, one should bear in mind that, particularly during the pre-monsoon season, high photochemical O_3 concentrations due to anthropogenic pollution and biomass burning strongly affect South Asia and the Southern Himalayas, as also observed at NCO-P (see Bonasoni et al., 2010). For the purpose of calculating the fraction of tropospheric O_3 due to SI at NCO-P, following Elbern et al. (1997), the integral stratospheric contribution O_{3S} was defined as:

$$O_{3S} = \sum_{i=1}^{n} \sum_{t=-T_i/2}^{T_i/2} O_3(t) \quad (1)$$

where for each season, $O_3(t)$ denoted the 30 min O_3 concentrations recorded during the *i*th event with time length T_i (expressed as number of 30 min values). The results, expressed as ppbv*h, are reported in Table 1. The O_{3S} seasonal cycle was characterised by maximum values during the pre-monsoon and dry seasons, minimum

ACPD
10, 1483–1516, 2010

values during the monsoon and post-monsoon, and a strong peak-to-peak amplitude (seasonal maximum to minimum ratio ≈26). This was in good agreement with the model experiment of Lelieveld et al. (2009), who showed a minimum of stratospheric originated O_3 during the summer period (July–September) over the Himalayas. The relative contribution of SI to the O_3 burden over the Southern Himalayas can be estimated by calculating the seasonal enhancement ratio between O_{3S} and the integral O_3 amount recorded outside SI (hereinafter O_{3NS}). The resulting values are reported in Table 2, where the seasonal enrichment ratios O_{3S}/O_{3NS} are expressed as percentages. Over the 2-year period, the average value of the enrichment ratio O_{3S}/O_{3NS} was 13.7%. The contribution of SI to the tropospheric O_3 as evaluated by the O_{3S}/O_{3NS} ratio shows a pronounced seasonal cycle, with a minimum during the monsoon (<0.1%), a maximum during the winter (24.2%) and intermediate but not-negligible values during the pre-monsoon (19.2%) and post-monsoon (12.6%).

6 Discussion and conclusions

The work presents the first 2-years (March 2006–February 2008) of continuous O_3 observations at the Nepal Climate Observatory – Pyramid (NCO-P, 5079 m a.s.l., Nepal). With the aim of contributing to clarifying the role played by transport processes in determining the O_3 levels and variability in one of the world's most critical high-altitude regions, a systematic assessment was performed of the influence of SI on O_3 concentrations recorded at this GAW-WMO station, which is considered representative of the Southern Himalayas remote troposphere. As O_3 is a powerful greenhouse gases and a dangerous pollutant and due to the increasing emissions of anthropogenic O_3 precursors over South Asia (Ohara et al., 2007), such activity appears to be particularly important also considering that this region is strongly influenced by the so-called Asian Brown Cloud, with severe implications on regional climate, air-quality and food security (Ramanathan et al., 2008).

As deduced from the analysis of 30-min average values (49±12 ppbv, N=31 420),

the seasonal O_3 behaviour was found to be characterised by a maximum during the pre-monsoon (61±9 ppbv, N=9376) and a minimum during the monsoon (39±10 ppbv, N=10 836) seasons. As shown by Bonasoni et al. (2010), such seasonal variation is partially influenced by the synoptic-scale atmospheric circulation related to the South Asia monsoon regime. In fact, during summer air-masses poor in O_3 were transported from lower latitudes to the Southern Himalayas, while during the pre-monsoon the measurement site was mostly affected by westerly air-masses originating from North Africa, Middle East, Central Asia and Northern India as well. In addition to long-range transport, the efficient day-time valley wind circulation can play an important role in transporting polluted air-masses rich in O_3 to NCO-P. Thus, the correct identification of the measurement periods influenced by such pollution transports is fundamental for quantifying the exact contribution of long-range transport processes (like SI) on the observed O_3 levels.

To identify the days possibly influenced by SI, analyses were performed of in-situ observations of O_3, RH, AP, satellite-derived OMI-TOC data and PV values provided by the LAGRANTO back-trajectory model. After defining an appropriate threshold value for each tracer, different selection criteria were applied to identify possible SI days at NCO-P. In summary, during the 2-year investigation, 14.1% of the analysed days turned out to be affected by SI. These results appeared slightly higher than showed in Cristofanelli et al. (2009) who used a similar approach for analysing one-year of data at the same measurement site, thus suggesting that our estimate of the SI frequency directly affecting South Himalayas is quite robust. Considering the high altitude of the measurement site (5079 m a.s.l.), the values may appear low, if compared with the SI frequencies (ranging from 5% to 40%) inferred at high mountain stations located in Europe (with altitudes ranging from 2100 to 3800 m a.s.l., see Stohl et al., 2000; Cristofanelli et al., 2006; Cui et al., 2009; Trickl et al., 2009). It could indicate that the Southern Himalayas is not among the world regions most affected by SI. On applying a less restrictive methodology, which excluded the threshold on O_3 concentrations (following Cristofanelli et al., 2006; Trickl et al., 2009), the occurrence of days affected by

ACPD
10, 1483–1516, 2010

SI increased to 30%. Nevertheless, our SI frequency estimate appears to be in good qualitative agreement with the modelling analyses performed by Sprenger and Wernli (2003), which showed that the probability of a deep SI affecting the NCO-P region is three time less than over Western and Central Europe, an area characterized by frequent cyclogenesis episodes and often directly impacted by the intense polar jet stream (e.g., Schuepbach et al., 1999; Sprenger and Wernli, 2003). Moreover, the Europe is located at the end of the North Atlantic storm track region, where PV streamer usually occur (Wernli and Sprenger, 2007). As deduced from the present analysis, a strong seasonal cycle characterizes the frequency of SI days with a minimum during the monsoon season (1.2%) and higher values during the rest of the year (21.5%). Bonasoni et al. (2010) showed that during non-monsoon seasons, the NCO-P area is significantly affected by westerly air-masses. Therefore, the results obtained here reflect the role of the SJS in promoting deep SI over the Southern Himalayas. In fact, during the summer monsoon the SJS is positioned on the northern side of the Tibetan Plateau (Schiemann et al., 2009; Ding and Wang, 2006), while from October to May the axis of the SJS is usually between 25–30° N. In particular, as shown by a companion paper (Cristofanelli et al., 2010), the presence of the upper tropospheric sub-tropical front, westerly moving disturbances and, quasi-stationary ridges represent the principal synoptic scenarios able to induce SI at the NCO-P during non-monsoon periods. On the other hand, the few SI events during the monsoon period are likely to be related to the occurrence of a monsoon depression over the Bay of Bengal and Northern Indian plains. Finally, with the aim of evaluating the occurrence of SI also in terms of events, time periods consisting of contiguous SI days were defined as "SI events": a total of 42 SI events were observed (19 during 2006 and 23 during 2007). The average time-length of the identified events was 2.3 days, with 80% of detected events having a time duration of less than 2 days.

With the aim of estimating the contribution of SI on O_3 levels at the NCO-P for the 2-year investigation period, the 30 min O_3, BC and RH data-sets were analysed. In particular, to prevent measurement periods possibly affected by anthropogenic trans-

ported pollution from influencing the estimate, data with high RH and BC, indicating the transport of polluted and wet air-masses by up-valley breezes, were not considered. On average, the days influenced by possible air-mass transport from the stratosphere showed a significant net O_3 increase of 27.1% (+13 ppbv) with respect to periods not affected by SI. In addition, the results indicated that the average net O_3 increases related to SI were characterized by a clear annual variation, with the highest values during the post-monsoon (+22.0%) and the lowest during the pre-monsoon (+8.6%). In order to calculate the fraction of tropospheric O_3 due to SI at NCO-P, the integral stratospheric O_3 contribution (O_{3S}) was calculated. Through this analysis it was estimated that 13.7% of surface O_3 recorded at NCO-P can be attributed to SI. On a seasonal basis, the lowest SI contributions were found during the summer monsoon (less than 0.1%), while the highest were found during winter (24.2%). Such values are in good agreement with the results of Sudo and Akimoto (2007) who, by running a tagged tracer simulation with a global chemical transport model, estimated that STE contributed from 10% to 20% of the annual TCO over the Southern Himalayas. However, it should be noted that the present estimates can vary if a different SI selection methodology is applied to screen SI at NCO-P. As an upper limit, on a yearly basis, about 30% of the O_3 observed at NCO-P can be tagged to SI, if O_3 thresholds were removed from the applied detection filters.

In the framework of the ABC project, the results presented contribute to filling the gap in knowledge concerning this important pollutant/regional greenhouse gas over the high Himalayas, providing the basis for a better evaluation of its contribution to the radiative forcing and air-quality in this critical region (Ramanthan et al., 2008). Based on the present estimates, during the non-monsoon seasons, SI can play a not-negligible role in determining the levels and variability of tropospheric O_3 over the Southern Himalayas, and therefore the radiative budget over the region. Thus, in evaluating future scenarios of climate variations, the influence of SI contributions to tropospheric O_3 cannot be omitted. However, other processes (e.g. long-distance and regional transport of air pollution, see Bonasoni et al., 2010; Marinoni et al., 2010) could play an

important role in determining O_3 levels over the Southern Himalayas. Further work will be deserved to investigate the contribution of polluted air-masses to the O_3 concentrations observed at NCO-P, thus providing up-to-date information on the role played by anthropic emissions in influencing O_3 variations in this important geographical area.

Acknowledgements. This study was carried out within the framework of the Ev-K^2-CNR Project. Part of the work was supported by ACCENT (GOCE-CT-2003-505337). The authors are grateful to EMPA-WCC for providing the travel standard used for intercomparing the NCO-P O_3 analyser on February 2007. The TOC-OMI data were produced with the Giovanni online data system, developed and maintained by the NASA Goddard Earth Sciences (GES) Data and Information Services Center (DISC). OMI mission scientists and associated KNMI and NASA personnel are acknowledged for the production of the data used in this research effort. Finally, the authors would like to thank the Nepalese staff working at NCO-P for their valuable work under very difficult conditions.

References

Agrawal, M., Auffhammer, M., Chopra, U. K., Emberson, L., Iyngararasan, M., Kalra, N., Ramana, M. V., Ramanathan, V., Singh, A. K., and Vincent, J.: Impacts of Atmospheric Brown Clouds on Agriculture, Part II of Atmospheric Brown Clouds: Regional Assessment Report with Focus on Asia, Project Atmospheric Brown Cloud, UNEP, Nairobi, Kenya, 2008.

Bonasoni, P., Evangelisti, F., Bonafè, U., Ravegnani, F., Calzolari, F., Stohl, A., Tositti, L., Tubertini, O., and Colombo, T.: Stratospheric ozone intrusion episodes recorded at Mt. Cimone during VOTALP project: case studies, Atmos. Environ., 34, 1355–1365, 1999.

Bonasoni, P., Laj, P., Angelini, F., Arduini, J., Bonafè, U., Calzolari, F., Cristofanelli, P., Decesari, S., Facchini, M. C., Fuzzi, S., Gobbi, G. P., Maione, M., Marinoni, A., Petzold, A., Roccato, F., Roger, J. C., Sellegri, K., Sprenger, M., Venzac, H., Verza, G. P., Villani, P., and Vuillermoz, E.: The ABC-Pyramid atmospheric research observatory in himalaya for aerosol, ozone and halocarbon measurements, Sci. Tot. Environ., 391, 241–251, 2008.

Bonasoni, P., et al.: Atmospheric brown clouds in the Himalayas: first two years of continuous observations at the Nepal-climate observatory at Pyramid (5079 m), in preparation, 2010.

Böhner, J.,: General climatic controls and topoclimatic variations in Central and High Asia, BOREAS, 35, 279–294, 2006.
Conti, S., Meli, P., Minelli, G., Solimini, R., Toccaceli, V., Vichi, M., Beltrano, C., and Perini, L.: Epidemiologic study of mortality during the summer 2003 heat wave in Italy, Environ. Res., 98, 390–399, 2005.
Cristofanelli, P., Bonasoni, P., Tositti, L., Bonafè, U., Calzolari, F., Evangelisti, F., Sandrini, S., and Stohl, A.: A 6-year analysis of stratospheric intrusions and their influence on ozone at Mt. Cimone (2165 m above sea level), J. Geophys. Res., 111, D03306, doi:10.1029/2005JD006553, 2006.
Cristofanelli, P., Bonasoni, P., Bonafè, U., Calzolari, F., Duchi, R., Marinoni, A., Roccato, F., Vuillermoz, E., and Sprenger, M.: Influence of lower stratosphere/upper troposphere (LS/UT) transport events on surface ozone at the Everest-Pyramid GAW Station (Nepal, 5079 m a.s.l.): first year of analysis, Int. J. Rem. Sens., 30(15), 4083–4097, 2009.
Cristofanelli, P., Bracci, A., Sprenger, M., Bonafè, U., Calzolari, F., Duchi, R., Marinoni, A., Roccato, F., Vuillermoz, E., and Bonasoni, P.: Case studies of stratospheric intrusions at the Nepal climate observatory – Pyramid (Himalaya, 5079 m a.s.l.): a synoptic-scale investigation, Atmos. Chem. Phys. Discuss., in preparation, 2010.
Cui, J., Sprenger, M., Staehelin, J., Siegrist, A., Kunz, M., Henne, S., and Steinbacher, M.: Impact of stratospheric intrusions and intercontinental transport on ozone at Jungfraujoch in 2005: comparison and validation of two Lagrangian approaches, Atmos. Chem. Phys., 9, 3371–3383, 2009, http://www.atmos-chem-phys.net/9/3371/2009/.
Danielsen, E. F.: Stratospheric-tropospheric exchange based on radioactivity, ozone and potential vorticity, J. Atmos. Sci., 25, 502–518, 1968.
Davies, T. D. and Schuepbach, E.: Episodes of high ozone concentrations at the earth's surface resulting from transport down from the upper troposphere/lower stratosphere, Atmos. Environ., 28, 53–68, 1994.
Ding, D. and Wang, T.: Influence of stratosphere-to-troposphere exchange on the seasonal cycle of surface ozone at Mount Waliguan in Western China, Geophys. Res. Lett., 33, L03803, doi:10.1029/2005GL024760, 2006.
Eisele, H., Scheel, H. E., Sladkovic, R., and Trickl, T.: High resolution Lidar measurements of stratosphere-troposphere exchange, J. Atmos. Sci., 56, 319–330, 1999.
Elbern, H., Kowol, J., Sladkovic, R., and Ebel, A.: Deep stratospheric intrusions: a statistical

assessment with model guided analysis. Atmos. Environ., 31, 3207–3226, 1997.
Fischer, H., Kormann, R., Klüpfel, T., Gurk, Ch., Königstedt, R., Parchatka, U., Mühle, J., Rhee, T. S., Brenninkmeijer, C. A. M., Bonasoni, P., and Stohl, A.: Ozone production and trace gas correlations during the June 2000 MINATROC intensive measurement campaign at Mt. Cimone, Atmos. Chem. Phys., 3, 725–738, 2003, http://www.atmos-chem-phys.net/3/725/2003/.
Forster, P., Ramaswamy, V., Artaxo, P., Berntsen, T., Betts, R., Fahey, D. W., Haywood, J., Lean, J., Lowe, D. C., Myhre, G., Nganga, J., Prinn, R., Raga, G., Schulz M., and Van Dorland, R.: Changes in atmospheric constituents and in radiative forcing, in: Climate Change 2007: The Physical Science Basis. Contribution of Working Group I to the Fourth Assessment Report of the Intergovernmental Panel on Climate Change, edited by: Solomon, S., Qin, D., Manning, M., Chen, Z., Marquis, M., Averyt, K. B., Tignor, M., and Miller, H. L., Cambridge University Press, Cambridge, UK and New York, NY, USA, 2007.
Fuhrer, J. and Booker, F.: Ecological issues related to ozone: agricultural issues, Environ. Int., 29, 141–154, 2003.
Gauss, M., Myhre, G., Pitari, G., et al.: Radiative forcing in the 21st century due to ozone changes in the troposphere and the lower stratosphere, J. Geophys. Res., 108, 4292, doi:10.1029/2002JD002624, 2003.
GAW: report of the WMO meeting of experts on the quality assurance plan for the Global Atmospheric Watch (GAW), Garmisch-Partenkirchen, Germany, 26–30 March, 1992.
Han, Z., Chongping, H., Libo, Z., Wei, W., and Yongxiao, J.: ENSO signal in total ozone over Tibet, Adv. Atmos. Sci., 18, 231–238, 2001.
Henne, S., Klausen, J., Junkermann, W., Kariuki, J. M., Aseyo, J. O., and Buchmann, B.: Representativeness and climatology of carbon monoxide and ozone at the global GAW station Mt. Kenya in equatorial Africa, Atmos. Chem. Phys., 8, 3119–3139, 2008, http://www.atmos-chem-phys.net/8/3119/2008/.
Hoek, G., Fisher, P., Brunekreef, B., Lebret, E., Hofsschreuder, P., and Mennen, M. G.: Acute effects of ambient ozone on pulmonary function of children in The Netherlands, Am. Rev. Respire. Dis., 147, 11–117, 1993.
Jacobson, M. Z.: Atmospheric Pollution: History, Science and Regulation, Cambridge University Press, Cambridge, UK and New York, NY, USA, 2002.
Klausen, J., Zellweger, C., Buchmann, B., and Hofer, P.: Uncertainty and bias of surface ozone measurements at selected Global Atmosphere Watch sites, J. Geophys. Res., 108(D19),

4622, doi:10.1029/2003JD003710, 2003.
Lelieveld, J., Hoor, P., Jöckel, P., Pozzer, A., Hadjinicolaou, P., Cammas, J.-P., and Beirle, S.: Severe ozone air pollution in the Persian Gulf region, Atmos. Chem. Phys., 9, 1393–1406, 2009,
http://www.atmos-chem-phys.net/9/1393/2009/.
Levelt, P. F., van Den Oord, G. H. J., Dobber, M. R., Malkki, A., Visser, H., de Vries, J., Stammes, P., Lundell, J. O. V., and Saari, H.: The ozone monitoring instrument, IEEE T. Geosci. Remote, 44, 1093–1101, doi:10.1109/TGRS.2006.872333, 2006a.
Levelt, P. F., Hilsenrath, E., Leppelmeier, G. W., van Den Oord, G. H. J., Bhartia, P. K., Tamminen, J., de Haan, J. F., and Veefkind, J. P.: Science objectives of the ozone monitoring instrument, IEEE T. Geosci. Remote, 44, 1199–1208, doi:10.1109/TGRS.2006.872336, 2006b.
Loring, R. O. J., Fuelberg, H. E., Fishman, J., Watson, M. V., and Browell, E. V.; Influence of a middle-latitude cyclone on tropospheric ozone distributions during a period of TRACE A, J. Geophys. Res., 101(D19), 23941–23956, 1996.
Marinoni, A., et al.: Aerosol mass and black carbon concentration at NCO-P (South Himalayas, 5079 m a.s.l.), Atomos. Chem. Phys. Discuss., in preparation, 2010.
Mickley, L. J., Jacob, D. J., Field, B. D., and Rind, D.: Climate response to the increase in tropospheric ozone since preindustrial times: a comparison between ozone and equivalent CO_2 forcings, J. Geophys. Res., 109, D05106, doi:10.1029/2003JD003653, 2004.
Miyazaki, K., Iwasaki, T., Shibata, K., Deushi, M.: Roles of transport in the seasonal variation of the total ozone amount, J. Geophys. Res., 110, D18309, doi:10.1029/2005JD005900, 2005.
Moore, G. W. K. and Semple, J. L.: High Himalayan meteorology: weather at the south col of Mount Everst, Geophys. Res. Lett., 31, L18109, doi:10.1029/2004GL020621, 2004.
Moore, G. W. K. and Semple, J. L.: A Tibetan Taylor cap and a halo of stratospheric ozone over Himalya, Geophys. Res. Lett., 32, L21810, doi:10.1029/2005GL024186, 2005.
Ohara, T., Akimoto, H., Kurokawa, J., Horii, N., Yamaji, K., Yan, X., and Hayasaka, T.: An Asian emission inventory of anthropogenic emission sources for the period 1980–2020, Atmos. Chem. Phys., 7, 4419–4444, 2007,
http://www.atmos-chem-phys.net/7/4419/2007/.
Olsen, M. A., Gallus, W. A., Stanford, J. L., and Brown, J. M.: Fine-scale comparison of TOMS total ozone data with model analysis of an intense midwestern cyclone, J. Geophys. Res., 105, 20487–20498, 2000.
Paoletti, E.: Impact of ozone on Mediterranean forests: a review, Environ. Poll., 144, 463–474,

2006.
Petzold, A., Kramer, H., Schönlinner, M.: Continuous measurement of atmospheric black carbon using a multi-angle absorption photometer, Environ. Sci. Pollut. Res., 4, 78–82, 2002.
Ramanathan, V., Agrawal, M., Akimoto, H., et al.: Atmospheric Brown Clouds: Regional Assessment Report with Focus on Asia, United Nations Environment Programme, Nairobi, Kenya, 2008.
Schiemann, R., Lüthi, D., and Schär, C.: Seasonality and interannual variability of the westerly jet in the Tibetan Plateau region, J. Climate, 22, 2940–2957, 2009.
Schoeberl, M. R., Douglass, A. R., Hilsenrath, E., et al.: Overview of the EOS-Aura mission. IEEE T. Geosci. Remote, 44, 1066–1074, doi:10.1109/TGRS.2005.861950, 2006.
Schuepbach, E., Davies, T. D., and Massacand, A. C.: An unusual springtime ozone episode at high elevation in the Swiss Alps: contributions both from cross-tropopause exchange and from the boundary layer, Atmos. Environ., 33, 1735–1744, 1999.
Sebald, L., Treffeisen, R., Reimer, E., and Hies, T.: Spectral analysis of air pollutants, Part 2: Ozone time series, Atmos. Environ., 34, 3503–3509, 2000.
Sprenger, M., Croci Maspoli, M., and Wernli, H.: Tropopause folds and cross-tropopause exchange: a global investigation based upon ECMWF analyses for the time period March 2000 to February 2001, J. Geophys. Res., 108(D12), 8518, doi:10.1029/2002JD002587, 2003.
Sprenger, M. and Wernli, H.: A northern hemispheric climatology of cross-tropopause exchange for the ERA15 time period (1979–1993), J. Geophys. Res., 108(D12), 8521, doi:10.1029/2002JD002636, 2003.
Sprenger, M., Wernli, H., and Bourqui, M.: Stratosphere-troposphere exchange and its relation to potential vorticity streamers and cutoffs near the extratropical tropopause, J. Atmos. Sci., 64, 1587–1602, 2007.
Stohl, A., Spichtinger-Rakowsky, N., Bonasoni, P., Feldmann, H., Memmesheimer, M., Scheel, H. E., Trickl, T., Hubener, S., Ringer, W., Mandl, M.: The influence of stratospheric intrusions on alpine ozone concentrations, Atmos. Environ., 34, 1323–1354, 2000.
Sudo, K. and Akimoto, H.: Global source attribution of tropospheric ozone: long-range transport from various source regions, J. Geophys. Res., 112, D12302, doi:10.1029/2006JD007992, 2007.
Tanimoto, H., Sawa, Y., Matsueda, H., Uno, I., Ohara, T., Yamaji, K., Kurokawa, J., and Yonemura, S.: Significant latitudinal gradient in the surface ozone spring maximum over East Asia, Geophys. Res. Lett., 32, L21805, doi:10.1029/2005GL023514, 2005.

Tian, W., Chipperfield, M., and Huang, Q.: Effects of the Tibetean Plateau on total column ozone distribution, Tellus B, 60, 622–235, 2008.
Trickl, T., Feldmann, H., Kanter, H.-J., Scheel, H.-E., Sprenger, M., Stohl, A., and Wernli, H.: Forecasted deep stratospheric intrusions over Central Europe: case studies and climatologies, Atmos. Chem. Phys. Discuss., 9, 2223–2288, 2009, http://www.atmos-chem-phys-discuss.net/9/2223/2009/.
Venzac, H., Sellegri, K., Laj, P., Villani, P., Bonasoni, P., Marinoni, A., Cristofanelli, P., Calzolari, F., Fuzzi, S., Decesari, S., Facchini, M.-C., Vuillermoz, E., and Verza, G. P.: High frequency new particle formation in the Himalayas, PNAS, 105(41), 15666–15671, 2008.
Wahid, A., Milne, E., Shamsi, S. R. A., Ashmore, M. R., and Marshall, F. M.: Effext of oxidants on soybean growth and yield in Pakistan, Environ. Poll., 113, 271–280, 2001.
Wang, T., Wong, H. L. A., Tang, J., Ding, A., Wu, W. S., and Zhang, X. C.: On the origin of surface ozone and reactive nitrogen observed at a remote mountain site in the Northeastern Qinghai-Tibetan Plateau, Western China, J. Geophys. Res., 111, D8, D08303, doi:10.1029/2005JD006527, 2006.
Wernli, H. and Davies, H.: A Lagrangian-based analysis of extratropical cyclones, Part I: The method and some applications. Quart. J. Roy. Met. Soc., 123, 467–489, 1997.
Wernli, H. and Sprenger, M.: Identification and ERA-15 climatology of potential vorticity streamers and cutoffs near the extratropical tropopause, J. Atmo. Sci., 64, 1569–1586, 2007.
West, J. J., Naik, V., Horowitz, L. W., and Fiore, A. M.: Effect of regional precursor emission controls on long-range ozone transport – Part 2: Steady-state changes in ozone air quality and impacts on human mortality, Atmos. Chem. Phys., 9, 6095–6107, 2009, http://www.atmos-chem-phys.net/9/6095/2009/.
Wild, O.: Modelling the global tropospheric ozone budget: exploring the variability in current models, Atmos. Chem. Phys., 7, 2643–2660, 2007, http://www.atmos-chem-phys.net/7/2643/2007/.
Wimmers, A. J. and Moody, J. L.: Tropopause folding at satellite-observed spatial gradients: 1, verification of an empirical relationship, J. Geophys. Res., 109, D19306, doi:10.1029/2003JD004145, 2004.
Wotawa, G., Kroger, H., and Stohl, A.: Transport towards the Alps – results from trajectory analyses and photochemical model studies, Atmos. Environ., 34, 1367–1377, 2000.
World Meteorological Organization (WMO): Atmospheric ozone 1985: global ozone research and monitoring report, WMO Rep. 16, Geneva, Switzerland, 1986.

Zanis, P., Schuenpbach, E., Gaeggeler, H. W., Huebener, S., and Tobler, L.: Factors controlling Beryllium-7 at Jungfraujoch in Switzerland, Tellus, 51(4), 789–805, 1999.
Zachariasse, M., van Velthoven, P. F. J., Smit, H. G. J., Lelieveld, J., Mandal, T. K., and Kelder, H.: Influence of stratosphere-troposphere exchange on tropospheric ozone over the tropical Indian Ocean during the winter monsoon, J. Geophys. Res., 105, D12, 15403–15416, 2000.
Zhu, T., Lin, W., Song, Y., Cai, X., Zou, H., Kang, L., Zhou, L., and Akimoto, H.: Downward transport of ozone-rich air near Mt. Everest, Geophys. Res. Lett., 33, L23809, doi:10.1029/2006GL027726, 2006.

Table 1. Identification of season transitions as a function of the local weather regime at NCO-P (from Bonasoni et al., 2010).

Year	Season	Start day–End day
2006	Pre-monsoon	1 Mar–20 May
	Monsoon	21 May–26 Sep
	Post-monsoon	27 Sep–20 Nov
2007	Winter	21 Nov 2006–31 Jan 2007
	Pre-monsoon	1 Feb–5 Jun
	Monsoon	6 Jun–12 Oct
	Post-monsoon	13 Oct–14 Nov
2008	Winter	15 Nov–18 Feb 2008

Table 2. SI at NCO-P: seasonal averaged O_3 concentration (O_3), O_3 excess (ΔO_3) and O_3 integral (O_{3S}). Seasonal averaged integral O_3 outside SI (O_{3NS}) and seasonal O_3 enhancement ratios (O_{3S}/O_{3NS}) at NCO-P are also reported.

Periods	O_3 (ppbv)	ΔO_3 (%)	O_{3S} (ppbv*h)	O_{3NS} (ppbv*h)	O_{3S}/O_{3NS} (%)
All seasons	61±9; *N*:3183	+27.1	9.7×10^4	7.0×10^5	13.7%
Pre-monsoon	65±9; *N*:1396	+8.6	4.5×10^4	2.4×10^5	19.2%
Monsoon	46±5; *N*:73	+18.0	1.7×10^3	2.2×10^5	<0.1%
Post-monsoon	55±5; *N*:373	+22.0	1.0×10^4	8.1×10^4	12.6%
Winter season	58±9; *N*:1341	+17.2	3.9×10^4	1.6×10^5	24.2%

ACPD
10, 1483–1516, 2010

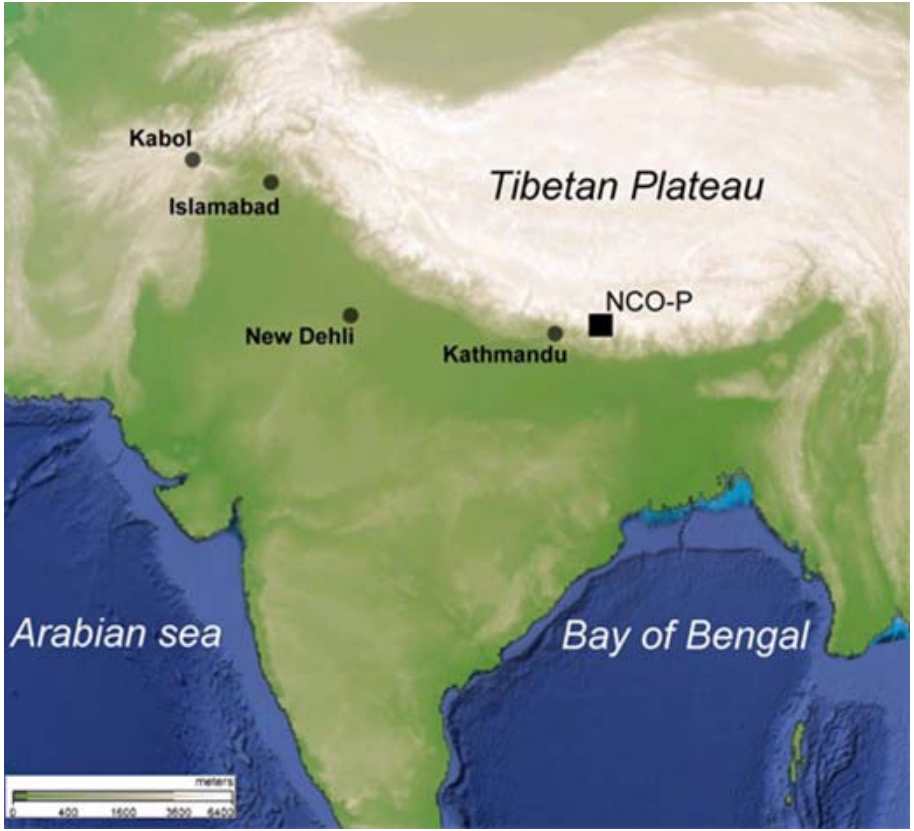

Fig. 1. NCO-P geographical location.

ACPD
10, 1483–1516, 2010

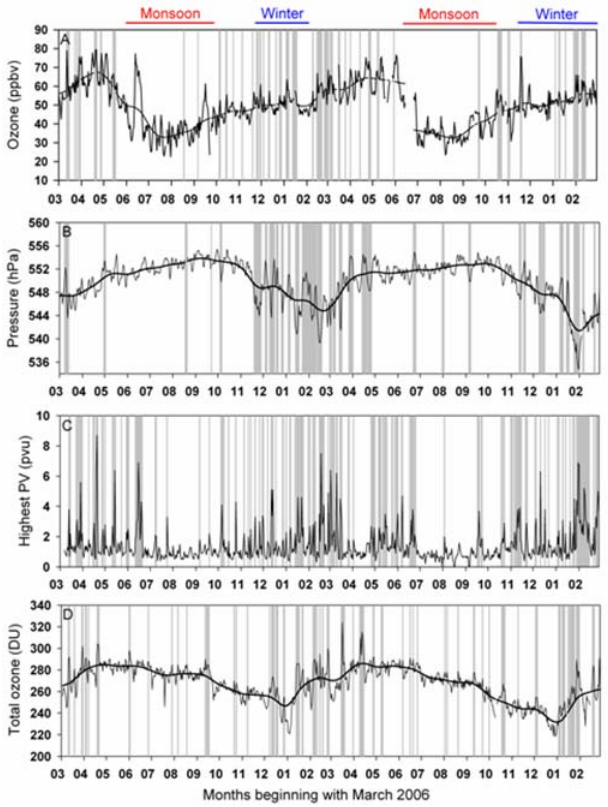

Fig. 2. Time series (daily average values) of surface O_3 **(A)**, atmospheric pressure **(B)**, maximum potential vorticity **(C)** and total ozone column **(D)** from March 2006 to February 2008. For surface O_3, atmospheric pressure and total O_3, the thick lines represent the seasonal behaviour obtained by applying the KZ filtering. The vertical grey bars denote the days characterised by parameter values exceeding the threshold for detection of SI events. Top horizontal coloured bars denote winter and monsoon seasons.

ACPD
10, 1483–1516, 2010

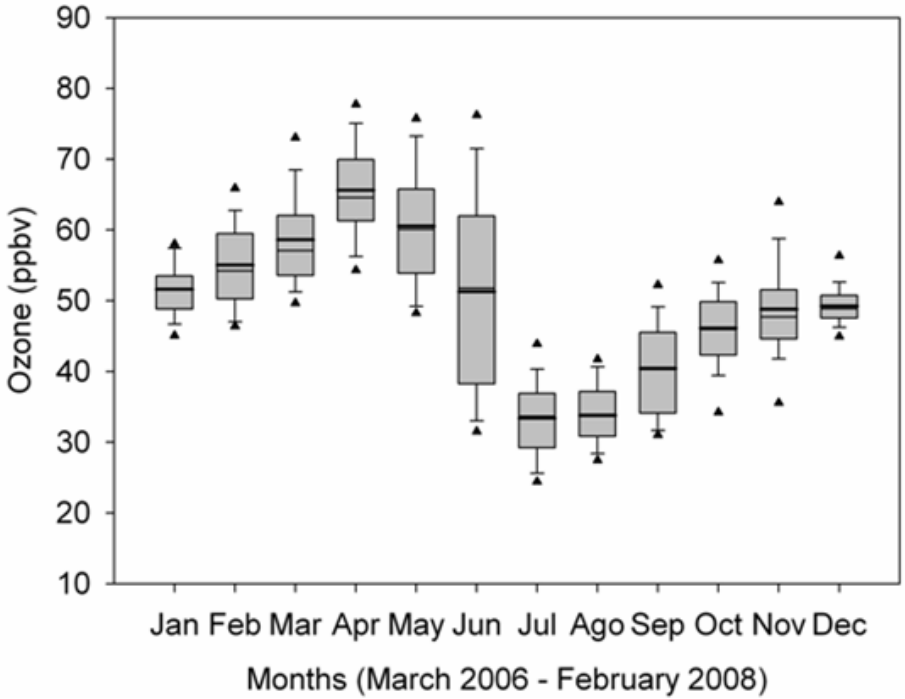

Fig. 3. Box-and-whiskers analysis of daily O_3 means for months from March 2006 to February 2008. The box and whiskers denote the 10th, 25th, 50th, 75th and 90th percentiles, the outliers the 5th and 95th percentiles and the bold lines the average values.

ACPD
10, 1483–1516, 2010

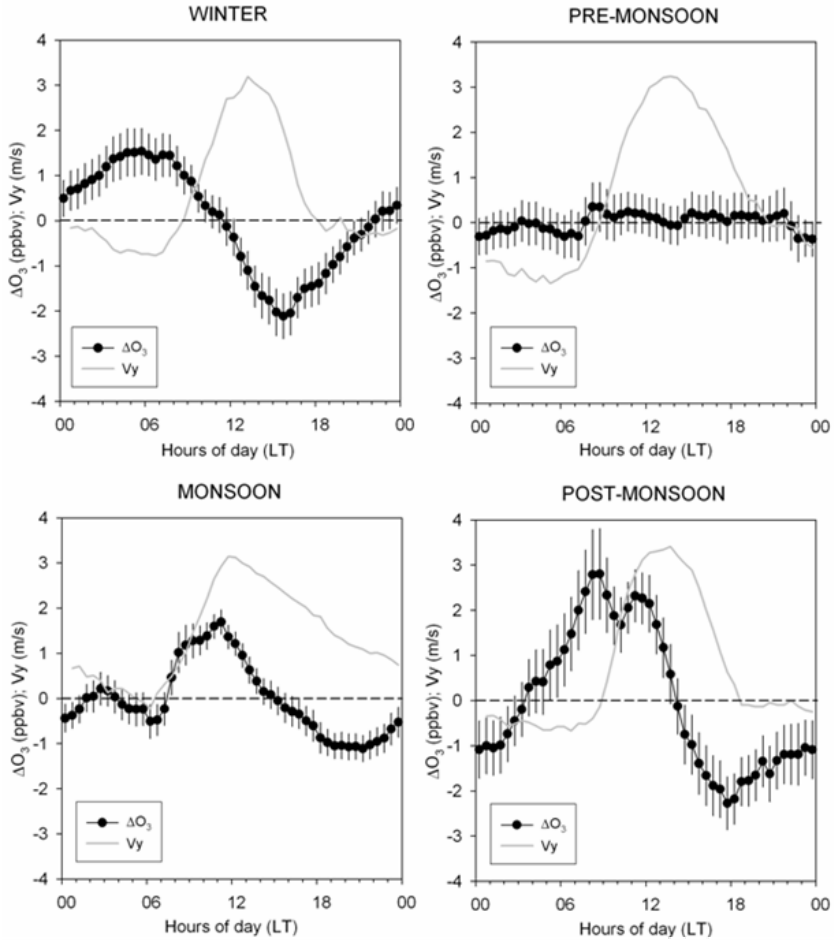

Fig. 4. Diurnal cycle of normalized O_3 values (ΔO_3) and meridional wind component (V_y) for the different seasons at the NCO-P. The vertical bars denote the 95% confidence level.

ACPD
10, 1483–1516, 2010

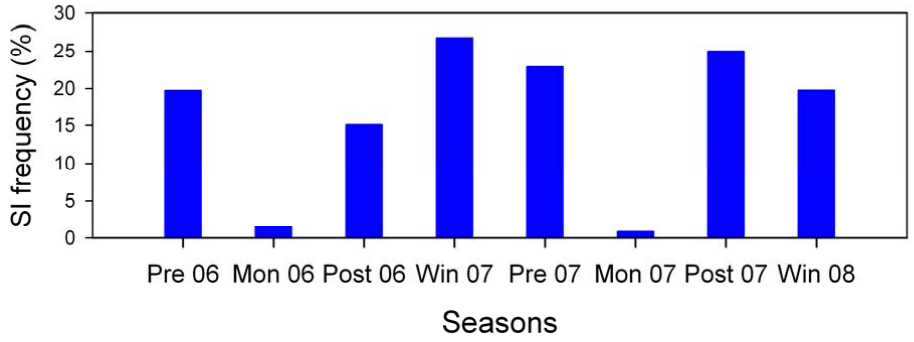

Fig. 5. Seasonal variation of SI frequency at NCO-P during the period March 2006–February 2008.

ACPD
10, 1483–1516, 2010

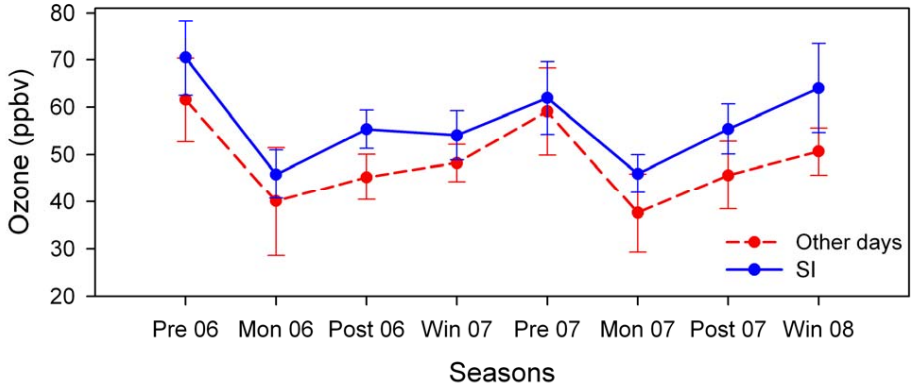

Fig. 6. Average O_3 concentrations recorded during SI and during periods not affected by SI (other days) at NCO-P for the period March 2006–February 2008. Vertical bars represent the standard deviations.

ACPD
10, 1483–1516, 2010